

Hybrid optimization of preparative chromatography for a ternary monoclonal antibody mixture

Vivien Fischer^{a,b}, Richard Kucia-Tran^b, Will Lewis^b, Ajoy Velayudhan^{a,*}

^a Dept. of Biochemical Engineering, The Advanced Centre for Biochemical Engineering, University College London, Bernard Katz Building, Gordon Street, London WC1H 0AH, United Kingdom

^b Biopharm Process Research, BioPharm R&D, GlaxoSmithKine, Gunnels Wood Road, Stevenage SG1 2NY, United Kingdom

* Corresponding author

Abstract

In the purification of monoclonal antibodies, ion-exchange chromatography is typically used among the polishing steps to reduce the amount of product-related impurities such as aggregates and fragments, whilst simultaneously reducing HCP, residual Protein A and potential toxins and viruses. When the product-related impurities are difficult to separate from the products, the optimization of these chromatographic steps can be complex and laborious. In this paper, we optimize the polishing chromatography of a monoclonal antibody from a challenging ternary feed mixture by introducing a hybrid approach of the simplex method and a form of local optimization. To maximize the productivity of this preparative bind-and-elute cation-exchange chromatography, wide ranges of the three critical operational parameters – column loading, the initial salt concentration and gradient slope – had to be considered. The hybrid optimization approach is shown to be extremely effective in dealing with this complex separation that was subject to multiple constraints based on yield, purity and product breakthrough. Furthermore, it enabled the generation of a large knowledge space that was subsequently used to study the sensitivity of the objective function. Increased design space understanding was gained through the application of Monte Carlo simulations. Hence, this work proposes a powerful hybrid optimization method, applied to an industrially relevant process development challenge. The properties of this approach and the results and insights gained, make it perfectly suited for the rapid development of biotechnological unit operations during early-stage bioprocess development.

Key words:

early-stage bioprocess development, antibody purification, preparative scale polishing chromatography, constrained experimental simplex optimization, design space

This article has been accepted for publication and undergone full peer review but has not been through the copyediting, typesetting, pagination and proofreading process, which may lead to differences between this version and the Version of Record. Please cite this article as doi: 10.1002/btpr.2849

© 2019 American Institute of Chemical Engineers

Received: Oct 30, 2018; Revised: Feb 01, 2019; Accepted: Apr 19, 2019

1 Introduction

Ion-exchange chromatography is a core technique used in the downstream processing of biopharmaceutical products and forms a major component of many purification platforms. In the purification of monoclonal antibodies (mAbs) it is typically deployed as a polishing step, playing an essential role in reducing the amount of impurities with similar physicochemical properties to the product, such as aggregates and fragments. Separations with three or more similar compounds in the feed are often complex and therefore typically require considerably more optimization than the initial mAb capture step. Examples of such process development efforts to achieve sufficient clearance from antibody aggregates are reported in the literature; ¹⁻⁵ examples of ternary separations involving aggregates as well as other product-related impurities are less frequent. ⁶⁻⁹ Other examples of ternary mixtures comprising non-mAb proteins, namely BSA, ovalbumin, cytochrome C and ribonuclease A, are commonly employed to study model-based optimization problems. ¹⁰⁻¹²

Finding optimal operating conditions for chromatographic separations is a complex optimization problem which needs to consider multiple inputs and multiple objectives to ultimately deliver a robust and economic process that produces drugs of highest quality and safety. In the early stage of process development, activities to identify effective operating conditions are restricted by tight timelines and limited feed stock. ¹³⁻¹⁵ This unique environment of early bioprocess development has inspired us to adopt the simplex algorithm as an *experimental* optimization method. Originally developed for the *numerical* optimization of functions by Spendley et al. in 1962 and later advanced by Nelder and Mead in 1965, ^{16,17} the simplex is a search algorithm that operates independently from a model, be it empirical or mechanistic, making it perfectly suited for iterative optimization based solely on experimental data. In this context, we define experimental optimization as a tool to rapidly optimize multivariate processes in high dimensional spaces whilst keeping the experimental cost low. The attractiveness of the simplex as an experimental optimization method is completely independent of its application for numerical optimization. Successful applications of the simplex in the experimental context are reported in the analytical field, ¹⁸⁻²² however, examples for the optimization of bioprocesses have been rare. ²³ Several case studies carried out by our group have demonstrated that the adaptive simplex method ¹⁷ and refined versions of it ^{24,25} were successful in identifying effective operating conditions for the downstream processing of proteins at the early development stage.

In this paper, we introduce a hybrid optimization method that combines the adaptive simplex method ¹⁷ with a form of local optimization which is demonstrated to be very effective in identifying favorable operating conditions from a large experimental space of input variables and subject to multiple constraints. This hybrid optimization method is applied in a case study for the ternary separation of a monoclonal antibody mixture with bind-and-elute cation-exchange chromatography in the gradient elution mode. In ion-exchange gradient elution, once an operating pH has been selected, the most important operating parameters are column loading, initial salt level and slope of the elution gradient (with flow rate as a somewhat less important parameter, depending on the resin). ¹⁵ Consequently, the three parameters loading, the initial salt level and gradient slope were varied, following an iterative and interactive

experimental strategy to maximize process productivity. With this approach, a large knowledge space was generated, and a robust and high-performing design space suggested based on Monte Carlo simulations. This work contributes to the scope of simplex applications by illustrating how it operates prospectively and in tandem with other techniques as a dynamic and efficient way to arrive at the optimum. In addition, it outlines some interesting features for the ternary separation of an antibody by polishing chromatography that could potentially be relevant for similar separations.

Accepted Article

2 Materials and Methods

2.1 Simplex Method

The adaptive simplex algorithm by Nelder and Mead¹⁷ is an iterative search method suitable for experimental optimization within defined constraints. It operates in the experimental space described by k independent variables or process inputs. Within this space, during the initialization, the simplex forms a geometric figure constructed from $k+1$ vertexes. For each vertex, the dependent variables or process outputs are evaluated with regards to their objective function value. This enables the simplex to be directed towards more favorable regions in subsequent steps and search for the optimum in the response surface. Movements of the simplex are controlled by a set of logical rules that compare and rank the vertexes regarding their output of two preceding iteration steps. Four basic movements allow the simplex to define the direction and adjust its size: reflection, expansion, contraction and shrink (Figure 1). Common to all movements is that the simplex is forced to migrate further or less away from the worst ranked vertex, whilst the total number of vertexes per step remains $k+1$. Constraints are a common feature of experimental optimization problems. In the simplex method, constraints for the inputs and outputs are readily implemented as penalties meaning a highly undesirable output is assigned to a vertex, leading to its rejection in the next iteration. For practical application the simplex method was implemented using VBA in Microsoft Excel (Microsoft Office 2016, Microsoft) and set to take direct inputs from the spreadsheet where the experimental information was recorded.

2.2 Case Study

A hybrid optimization approach of the simplex method is explored in the following case study, optimizing the loading and elution conditions of an industrially relevant antibody in a three-component system with bind-and-elute cation-exchange chromatography (CEX). The study was conducted in the context of early stage downstream process development, where finding process condition that maximize productivity, here the mass of recovered monomer protein per cycle time, with limited research resource is a key goal. It demonstrates how the simplex as an empirical technique can be used prospectively and in a truly experimental fashion. In addition, local fitting is investigated as a modelling tool to enhance the simplex search and rapidly populate large experimental spaces and its boundaries that emerge from multiple constraints. Knowledge gained during the optimization is further exploited with Monte Carlo simulations.

2.2.1 Feed Material

The product of interest was a monoclonal antibody from CHO (Chinese Hamster Ovary) cell culture, with aggregate levels of $\sim 8\%$ following Protein A capture. A lesser-retained impurity, i.e. a second mAb at $> 98\%$ monomer purity, produced in CHO cells, was added at $\sim 9\%$ concentration to generate the ternary feedstock used in the study. The difficulty of this separation was underlined by pairwise selectivities of no greater than 1.1, calculated from a low-loading ($2 \text{ g/L}_{\text{resin}}$) run, eluting the product with a linear gradient

starting from 30 mM initial salt concentration and a gradient slope of 15 mM/CV. In all experiments, the feed was adjusted to pH 5.0 and had a total concentration of 8.6 g/L.

2.2.2 Chromatography Experiments

The experiments were performed on a benchscale Äkta Avant system (GE Healthcare, Uppsala, Sweden) using pre-packed OPUS Minichrom columns (Repligen, Ravensburg, Germany) with a column volume of 5.03 mL, inner diameter of 0.8 cm and a bed height of 10 cm. The strong cation exchanger Eshmuno CPX (MMD Millipore, Darmstadt, Germany) was selected following the screening of potentially suitable cation and anion-exchange as well as mixed mode resins. A sodium acetate buffer system with ionic strengths of 25 mM (Buffer A) and 500 mM (Buffer B), pH 5.0 was used (all chemicals from Sigma-Aldrich Company, Dorset, UK unless specified otherwise). Conductivities were 4 mS/cm and 25 mS/cm respectively. For the elution, a linear salt gradient with different initial salt concentrations and gradient slopes was employed. The initial salt level was adjusted during a post-load re-equilibration step following sample injection. The flow rate was 200 cm/h in all steps but reduced to 100 cm/h during column loading. The sequence of steps was programmed in Unicorn software version 6.1 (GE Healthcare, Uppsala, Sweden). During the elution phase, 1 mL fractions were collected in 96-well deep well plates (VWR Collection, Lutterworth, UK) and analyzed for concentration and purity profile. The mass balances were accurate (97 ± 2 %), calculated based on the total protein recovery throughout the elution phase and during the re-equilibration step if product breakthrough occurred.

2.2.3 Analytical Methods

The concentration of total protein in the elution fractions was determined spectrophotometrically using a Tecan Magellan Infinite M200 microplate reader (Tecan Group Ltd, Männedorf, Switzerland). Sample preparation was performed on a Tecan Evo 200 platform (Tecan Group Ltd), controlled by Evoware software version 2.6. 200 μ L of sample per fraction were measured in flat bottom 96-well UV-STAR microplates (Greiner Bio-One, Stonehouse, UK). Absorption was measured at 280 nm, and path length correction applied to account for the volume of the microwells. Contamination of samples with DNA was not tested but is considered negligible since DNA is not expected to bind strongly to a CEX resin; further, the mass balances were accurate. Purity was assessed by SE-HPLC using a TSKgel G3000SW XL column (Tosoh Bioscience Ltd, Reading, UK) and a PBS-based mobile phase on an Agilent 1100 system (Agilent Technologies, Stockport, UK).

2.2.4 Objective Function

The objective of the optimization was to maximize the productivity of the CEX chromatography step as a function of column loading, the salt concentration at the start of the gradient (further referred to as 'initial salt') and the gradient slope. This functional relationship is expressed in Equation 2.1 as maximizing the recovered mass of the monomer product whilst minimizing the time required per chromatography cycle.

$$\max f(\text{Loading}, \text{Initial Salt}, \text{Slope}) = \max \left(\frac{\text{Monomer Mass}}{\text{Cycle Time}} \right) \quad (2.1)$$

The cycle time was defined as the time from the start of the pre-load equilibration phase, until the time point when the last fraction of interest in the elution pool was collected. Therefore, the cycle time did not account for cleaning and storage steps which are not normally on the critical path involved in the making of the product. Values of the objective function were recorded in typical units of productivity, scaled to the volume of the column as [g product/(h L_{resin})]. During the simplex optimization a modified objective function, measured in [mg/min], with higher sensitivity for yield was employed (Equation 2.2). The monomer yield was calculated as the percentage of mass of the monomer protein recovered in the pool per total mass of protein loaded.

$$\max f(\text{Loading}, \text{Initial Salt}, \text{Slope})^* = \max \left(\frac{\text{Monomer Mass} \cdot \text{Monomer Yield}}{\text{Cycle Time}} \right) \quad (2.2)$$

The optimization was subject to constraints representing the quality of the separation, i.e. purity and in some cases monomer yield. The purity of the chromatographic pool was required to be no less than 95 % (except in section 3.4 where the sensitivity of the objective function to different levels of purity was studied). In the determination of the objective function, the pool size played a central role and constituted an intermediate level of optimization, affecting the cycle time as well as product purity and yield. The relevant fractions were determined by reducing the pool size systematically from both ends of the elution peak, simulating all possible pooling options and selecting the pool that maximized product mass. Bounds on the input variables were imposed during the initial phase of the optimization.

2.2.5 Design of Experiments

A standard Design of Experiments (DoE) approach was initially employed as a scouting method, building a Central Composite design matrix in Design-Expert 10 (State-Ease, MN, USA) for low to moderate loading and high initial salt concentrations. In the design process, the elution endpoint was fixed to 381 mM salt (75 % Buffer B) for a 10 CV gradient. pH was included in the factor space. By conducting the first subset of five design experiments (Table 1) it was soon realized that the performance of the DoE points was low compared to the simplex points and consequently the DoE study was not completed. It is important to note that DoE methods play no further role in the results presented hereafter. However, the hybrid method developed here can use all experimental data, and so these five DoE points were added to the total dataset (naturally such a small dataset did not play an important role in the overall process).

2.2.6 Polynomial Fitting

Experimental data collected during the hybrid approach was fitted using second order polynomials to gain localized insight into primary trends of the objective function and to model the responses of improving quality as process knowledge increased. Reduced hierarchical models (p-value < 0.1) were generated for

the individual outputs (monomer mass, monomer yield and cycle time) via least square regression. The individual models were then multiplied to produce the objective function in Equation 2.1.

2.2.7 Monte Carlo Simulation

Monte Carlo Simulation^{26,27} enables the in-silico sampling and probabilistic analysis of process responses. In the case study, the simulations assumed that the process inputs are subject to uncertainty which can originate from limitations of the measurements and operating equipment and other sources of process variation. In the case study, polynomial models (section 2.2.6) were employed to approximate the process response as a function of the process inputs. This allowed the simulation of a large number of experiments, whose results clarified the robustness of the chosen operating conditions. Different design spaces or windows of operation were assessed during the simulation. Each design space was defined by the three process inputs loading, initial salt and gradient slope with a mean (or center point) and value for variability to reflect the uncertainty in the inputs at 3-sigma level. The inputs were assumed to be normally distributed around mid-point of the design space and across a sample size of 1000. The normally distributed inputs were generated using the random sample generator *randn* in Matlab 2016a (The MathWorks® Incorporated, MA, USA) and the process responses returned as the function values of the polynomial models.

3 Results and Discussion

3.1 Overview of Hybrid Approach

To optimize the operating conditions for the polishing of a monoclonal antibody mixture, aiming to maximize the productivity of the CEX chromatography step, a hybrid approach was investigated in two stages:

- i) Adaptive simplex optimization
- ii) Exploratory stage with local fitting (regression of experimental data)

The hybrid approach was employed to find an optimal window of operation within the experimental space of the three input variables: column loading, initial salt concentration and gradient slope. These inputs are often the most influential parameters in preparative chromatography, apart from pH, and are thus investigated and optimized most commonly during early stage purification development. Purity was not included as an optimization variable, and instead functioned as a constraint with a fixed target value of $> 5\%$. In addition, constraints for yield were introduced during the optimization and their impact on the optimum was analyzed. The implementation of such constraints as penalties is described in methods, section 2.1.

In the first stage of the approach, the adaptive simplex method (methods section 2.1) was used to rapidly move towards promising parameter conditions. The strength of the simplex algorithm in its role as an experimental optimizer (and in contrast to the more common application for numerical optimization) is based on its ability to explore multi-dimensional spaces efficiently and at low experimental cost of one or two additional points per iteration. The iterative procedure is flexible and allows the experimenter to use new information immediately; thus, if the past few runs seem to indicate slow progress in a region where the performance is not high, the current simplex can be stopped, and a new simplex started elsewhere. This adaptability is very useful in early process development, where process understanding is initially limited, and is more efficient than conventional DoE methods, which cannot be stopped in the middle of a run. In this study, it will be seen that the rapid adaptation of our hybrid method to the locus of product breakthrough was critical to rapid optimization.

Local fitting, here the regression of experimental data, was used as a technique to visualize trends in the experimental space under investigation. The regression models were progressively refined by adding data points a) delivered by the simplex as it continued to advance to areas of increasing objective function value and b) by picking data points following the simplex' trend and along the boundaries or extremes of the experimental space, subsequently referred to exploratory points. The experimental outline of both stages is described in detail in the following sections and implications of the approach are discussed in the dedicated section 3.5. In a separate follow-up study, Monte Carlo simulations were used with the

regression models to study trade-offs and robustness of the objective function and to select an optimum window of operation.

Note that DoE data played a minimal role in this study, as discussed in 2.2.5. However, the proposed hybrid approach can use all forms of experimental data. Although the DoE study was not completed, the data was not lost and contributed to refine the regression models at the exploratory second stage of the hybrid approach.

3.2 Adaptive Simplex Method

In the first stage of the optimization, the simplex was initialized within a subset of the experimental space that represented typical, though nonetheless conservative, values for the operation of a difficult CEX step and provided a starting point for the optimization. Initially, the input variables were defined to lie within specified intervals, narrowing the search space to [10, 50] mM/CV for the gradient slope, [25, 50] mM for the initial salt, and [15, 40] g/L_{resin} for column loading. In this three-dimensional space spanned by the input variables, the first simplex is prescribed by the four points connected by dashed lines in Figure 2a. The first vertex at average loading accompanied by a long and shallow gradient was adopted from earlier resin scouting studies (data not show), and the remaining three simplex vertexes were scattered around this point within $\pm 20\%$ of the column loading and the initial salt concentration, and $\pm 50\%$ of the gradient slope. The simplex was driven by the objective function in Equation 2.2, described as the product of recovered monomer mass per cycle time with additional emphasis on yield (in the following abbreviated m_{rec}/T). This modification was intended to help shape the objective function and increase the sensitivity of the optimum, granting product mass a higher importance or weighting over time.

In this simplex-dominated phase of the optimization, the simplex searched the permitted space rapidly, exploring 54% of the space in 10 iterations following the path numbered in Figure 2a. Throughout the optimization, the simplex steadily increased the column loading, building a sufficiently large data set in the first four iterations to encourage loosening the loading boundary of 40 g/L from iteration five onwards. This gave room for an additional 29% loading to be explored by the simplex. Assessing the changes in the output variables from iteration one to five revealed that the simplex repeatedly explored areas of $< 70\%$ yield in favor of increasing slopes (average increase 13%) and dropping cycle times (average reduction 25%). At this point, a yield constraint of $\geq 70\%$ was introduced and the simplex re-initialized from four of the existing points which satisfied the new output constraint. Such adjustments to the input and output variable ranges were easily implemented in the simplex method and are indicative of the simplex's flexibility and ability to adapt to varying experimental spaces as more process insight is gained.

In subsequent iterations and subject to the yield constraint, the final value of the objective function increased by 19% compared to the best response from the initial simplex in iteration one. This moderate increase in productivity led to the identification of an operating "sweet spot" close to the boundaries of the constrained space in a total of 13 chromatography experiments; one experiment per iteration in addition to three experiments to initialize the simplex at the beginning of the optimization. Within the

predefined conventional yet reasonable boundaries, and against initial expectations, an internal optimum was not determined. The simplex was halted because no further improvement of the objective function was expected within the set boundaries.

3.3 Hybrid Optimization with Local Fitting

The simplex optimization led to two main conclusions: a) For the optimization much larger ranges of the input variables had to be considered against initial assumptions; and b) a positive trend for the objective function was associated with higher column loading. These observations motivated the decision to widen the experimental space beyond the input variable limits applied during the simplex search. The purpose of the second stage of the hybrid optimization approach was therefore to rapidly explore the resulting vast experimental space by testing variable combinations in promising areas and by studying directions of high potential with local fitting. The nature of the exploratory points was unstructured, providing only very localized information. Here, local fitting enabled us to gain insight into the underlying trends of the entire available data, comprising the simplex points and a growing number of exploratory points. Those trends were used as a guide to help identify promising settings for the input variables and to populate areas of interest.

The first exploratory points were collected at very high loading, following the trend indicated by the simplex. Points at high initial salt conditions were also considered based on the outcomes of a partial DoE study that was conducted in the high salt regime as suggested by a standard DoE approach. However, this DoE study was not completed since it was soon realized that the chosen factor ranges would be sub-optimal. Both directions, moving towards high load and high initial salt concentrations, resulted in an increase of the objective function. Following those trends to increase the objective function even more, however, would inevitably lead to product breakthrough (BT) becoming a limiting factor and experimental constraint, re-defining the applicable experimental space. Further exploratory points were added one-by-one that enabled the identification of the product breakthrough curve with minimal experimental effort. The final set of 34 data points and the BT boundary are depicted in the scatter plot of Figure 2b.

From the data set (simplex points, exploratory points and available DoE points), second order polynomial models were generated to visualize the objective function in Equation 2.1, describing the recovered product mass per cycle time (abbreviated M/T). This was not only a more intuitive way of writing the objective function; as more process insight was gained, it also became clear that the optimum was disproportionately controlled by time and therefore the additional weighting of mass (Equation 2.2) had a negligible effect (discussed in section 3.4). The objective function is illustrated in two dimensions in Figure 3, holding the respective third variable at three selected set-points. The corresponding regression model showed no significant lack of fit and good values for $R^2 = 0.92$ and adjusted $R^2 = 0.90$. The information is complemented by the re-constructed preparative chromatograms in Figure 4.

The BT curve was an important element of the objective function M/T visualized in Figure 3 since it defined a physical boundary that altered the behavior of the process. To mark the transition, a polynomial function of the inputs loading and initial salt was fitted for 10 data points of up to 10 % BT and for slopes varying from 12 to 35 mM/CV (median 15 mM/CV). The fit of the BT curve produced reasonable values for R^2 and adjusted R^2 of 0.90 and 0.85, demonstrating no lack of fit. Since only a small window of slopes was studied with regards to BT, the BT curve is reduced to a constant straight line in those graphs where slope is a variable.

To estimate the impact of BT on productivity, two extreme scenarios are presented in Figure 3. In the first case (Figure 3-I), no specific BT model is applied; this represents the ideal scenario of a process that is unaffected by BT. The second case (Figure 3-II) describes the worst-case scenario assuming that all the product breaking through prior to the start of the elution gradient, is lost in the process. Although this scenario can be regarded as a more realistic approximation of the objective function, in practice it is unlikely that the product breaking through with the lesser retained impurity is lost to the same extent in the final pool of the product. This is exemplified by the chromatogram in Figure 4c. Hence, both representations of product BT must be interpreted with caution. For all following illustrations of the objective function, the worst-case scenario for product BT will be applied.

For the areas not affected by BT, some general observations can be summarized. In the panel of Figure 3-II loading stands out as the most significant input variable; an observation that is particularly appreciable by comparing the color scales of Figure 3-II (g-k). A similar, although less pronounced, trend is seen in Figure 2-II (a-f) showing a larger incremental gain for loading over the initial salt concentration and even more so over slope. Simultaneously, as the loading increases, yield drops. In Figure 4 a) and d) this is illustrated by a larger integral of the product in the pool when more protein is loaded. This however leads to increasingly mixed fractions on both sides of the product peak, negatively affecting the purity of the pool and consequently yield. The strongest dependency of yield is seen in relation to different gradient slopes (Figure 3-II, d-k). With increasing slopes, the peaks in Figure 4 b) become narrower, resulting in a higher level of contamination on either side of the product peak and higher sensitivity for loading. The reduction in cycle time balances the effect of higher loadings and creates a sweet spot for operating slopes between 15 and 30 mM/CV. Cycle time is effectively reduced by a second variable: In chromatogram Figure 4 b) increasing the initial salt has the immediate advantage of forcing the product to elute very soon after the gradient started. This effect is highly influential in shaping the objective function in Figure 3-II (a-c) that would otherwise increase (almost) linearly with loading.

Overall process productivity is governed by two variables – the initial salt concentration that mainly controls cycle time and loading that mainly controls the recovered product mass. It is these characteristics of the objective function that lead to an optimum that is primarily determined by the BT curve as a physical constraint, in addition to constraints imposed on yield. This significant impact of BT on process productivity was a surprising feature of the separation and highlighted the importance of widening the input variable ranges for less traditionally behaved molecules to find optimal conditions, even when it meant to extend the search towards the physical limits of the experimental space. Further analysis of the objective function

will focus on the 2D plane of the input variables loading and initial salt that have shown to be the most influential factors in this separation.

3.4 Performance and Sensitivity of Different Objective Functions

The previous analysis of the regression models showed that optimal process productivity is not only dependent on the input variable settings but also governed by the physical boundary of product breakthrough and constraints for yield. The sensitivity of the objective function M/T with respect to those findings was investigated **(I)** by evaluating the impact of changing targets for purity. Moreover, different objective functions were studied with regards to sensitivity and performance **(II)** by prioritizing recovered mass over cycle time, by increasing the exponent of mass and thus applying a higher weighting in the objective function M^3/T and **(III)** for an objective function that is reduced to mass only by creating an overlay with the isolines for yield and cycle time. Pools with 90 %, 95 % and 98 % purity were simulated using the analytical information of the individual elution fractions for the collected data of each chromatography run. Based on the simulated optimal pools, polynomial models for product mass and cycle time were generated to calculate the different objective functions.

(I) For the objective function M/T (Figure 5 a–c), increasing the purity requirements led to lower productivities. This was to be expected as mixed fractions close to the boundaries of the pool forced a tighter cut of the pool in order to meet the purity requirement, resulting in generally smaller pool sizes and overall lower yields. At high loadings, the effect of fraction mixing was enhanced, causing the optimum to shift leftward. **(II)** When monomer mass was assigned a higher weighting (M^3/T , Figure 5 d–f), achieving high response values was more heavily dependent on loading and less on the initial salt, ultimately pushing the optimum further towards high loading regimes. **(III)** The contour plots in (Figure 5 g–i) show the objective function for mass. Yield and cycle time are plotted as separate sets of isolines. This representation of mass plotted with constraints reveals some key characteristics of the separation with regards to the loading and initial salt. Column loading took a primary role in increasing mass, whilst the initial salt concentration functioned predominantly to reduced cycle time. This effect of the initial salt was stronger than initially thought, and critical in defining the curvature that shapes the optima in Figure 5 (I).

By focusing on mass only, Figure 5 (III) can be interpreted as process performance maps that could be employed to inform about preferable operating conditions, targeted at different scenarios such as higher requirements for purity to compensate for potential issues with the shelf life of a drug product. In other scenarios saving cycle time could become an important factor, for example when experiments are conducted at bench scale, or when other classes of therapeutics, like small molecules, with rapid turnover times are considered. Under these circumstances, performance maps of this kind would enable scientists to respond flexibly to changing priorities in the development and supply of drug products.

3.5 Considerations of a Data-Driven Hybrid-Optimization Strategy

The proposed hybrid optimization method builds on the strength of the simplex to facilitate a data-driven holistic approach in identifying conditions of maximum process performance. Advantages of the simplex algorithm stem from its ability to rapidly search and evaluate potential process conditions following an interactive optimization routine. The iterative nature of the algorithm means that inputs from different data sources and operator suggestions can be incorporated on-the-fly, promoting the algorithm to operate flexibly and prospectively. These properties of the simplex method create opportunities for interactive workflows in tandem with other techniques such as local fitting.

Central to the hybrid approach is the idea of systematically taking stock of all the available data and increasing process insight as the optimization progresses. The simplex is a hill climbing method that navigates based on experimental data and finds optima with high likelihood and accuracy^{24,28}. The performance of the simplex depends on the path leading to the optimum and varies, for example, with the starting location, the distance from the optimum or constraints encountered with respect to operational parameters. It has been shown to cope with noisy data along its path and correct previously measured points of high variability by readjusting the path towards the true optimum.²⁹ In the best case, this path can follow a distinct and clear trend or it may be less defined. In the latter case, the simplex might require more time to assess surrounding areas before settling in a specific direction, especially if changes in the objective function are only small. Here, the optimization can be enhanced by supplementing the simplex and assessing additional points further away from the searched areas. Such exploratory points can be picked by eye or selected based on local fitting as a tool that allows the quantification of exploratory data and provides insight into underlying trends. Of particular interest are those points that lead to rapid changes in the objective function or that describe non-feasible settings for operational variables.

Local fitting forms the second element that contributes to the hybrid character of the optimization approach. The fits are based on unstructured, non-uniform data that is progressively refined as more exploratory data is added. From a sufficiently sized data set, global fits can be generated to represent the objective function. This approach, however, is different from the regression models typically used as part of a traditional DoE methodology, which is instead based on fixed experimental designs in a defined area of the operational space and with data structured to enable statistical analysis. In the hybrid approach, unstructured data is fitted to enhance the simplex by deciding whether to continue the simplex, or move it to a different area. Whilst the current study did not lend itself to a detailed discussion of DoE and the simplex method, comparisons of both methods have been considered elsewhere in literature published by our group.^{24,25,28}

For different types of optimization problems, the two elements of the hybrid approach – simplex algorithm and local fitting – can hold varying importance. Where the problem is strongly controlled by constraints, as in the case of product breakthrough in the current study, it is paramount to outline the constraints rapidly. In this special case, picking points to delineate the boundary is superior to running the simplex as usual,

which is more likely to require multiple steps because several of them will fall beyond the BT curve. Here, the BT curve was characterized using local fitting based on a minimum but sufficient number of data points. To guarantee high process productivity, the process was forced to operate as close as possible to the BT constraint. Hence, in the *highly constrained scenario*, there was no further room for optimization. This is conceptually different from the *less constrained case*, where sequential operation of the simplex is profitable and workflows form an interplay of sampling large experimental spaces and initializing sequential simplex searches by including high-performing external data points as areas of interests become more defined. The ability to change between both elements of the hybrid approach provides a powerful tool that can be tailored to effectively find the optimum settings of the operational inputs.

3.6 Monte Carlo Simulation and Design Space Definition

Detailed studies of the objective function, in addition to the large knowledge space generated during the optimization phase, facilitated probabilistic analysis to suggest an optimal and robust design space. In this case study where process performance was highly controlled by the constraint of product breakthrough and targets for yield, Monte Carlo simulations provided a structured way of assessing the impact of variability in the process inputs on overall design space performance and the reward by accepting a risk of failing the constraints.

Based on traditional assumptions and as a starting point for the Monte Carlo simulations, an initial design space was located in the productivity landscape of Figure 6 to satisfy a yield target of 70 % and avoid product breakthrough. The resulting design space was specified by (39 ± 3) g/ L_{resin} loading, (145 ± 10) mM initial salt and (20 ± 5) mM/CV gradient slope. During the simulation, the initial design space was moved by one quarter of its size, along the two-dimensional grid depicted in Figure 6. The simulations included areas with up to 5 % BT based on the worst-case scenario for BT discussed in section 3.3. For every design space location in the grid, the productivity was calculated for 1000 random samples and evaluated against acceptance criteria for BT and/or failure to meet a defined yield constraint. Table 2 summarizes the simulation results comparing the initial design space with the optimal design spaces for three sets of acceptance criteria; these design spaces are illustrated in Figure 6.

The assessment of the Monte Carlo simulation results showed that the initial design space gave productivities of $20.5 \text{ g} \pm 0.4 \text{ g}/(\text{h } L_{\text{resin}})$, however, failed to maintain yields $\geq 70 \%$ in $\sim 1/3$ of the 1000 simulations. This behavior can be attributed with variations in the gradient slope that had not been accounted for when the design space was selected based on the pure graphical parameters of the productivity plots in Figure 6 for a constant value of the slope at mid-range.

The set of conditions for “Design Space 1” (Figure 6a) tried to improve the robustness of the initial design space by reducing the risk of failing the yield constraint of 70 % and the chance of BT to 2 %. The criteria

were effective in producing a design space with median yields of 72.5 %. Improving the robustness of the design space reduced the productivity of the separation significantly by 25 % to 15.4 ± 0.6 g/(h L_{resin}).

The trade-off between yield and productivity was analyzed by proposing conditions that would produce a robust design space accepting zero risk to fail the acceptance criteria, however, lowering the yield requirements by 5 % to 65 % (Figure 6b). As a result, productivities increased by nearly 50 % from 15.4 g/(h L_{resin}) to 22.9 ± 0.3 g/(h L_{resin}) by giving up on average 4 % yield, comparing “Design Space 1” and “Design Space 2”. This resulted in a positive net-trade-off in favor of “Design Space 2”. For a comprehensive evaluation of trade-offs and to make the best possible design space choice other criteria such as cost and capacity of associated upstream and downstream steps could influence the decision process and should be considered.

The third and last design space was simulated without constraints for yield or BT in order to explore the maximum possible productivity (Figure 6c). By placing the “Design Space 3” entirely in the BT region, highest productivities of 25.3 ± 0.1 g/(h L_{resin}) were achieved. At the same time yields dropped to 63 % on average. For this design space to become a realistic and viable option, more characterization of the BT region would be required and additional experiments would need to be performed.

Ultimately the design space selection process must consider various criteria relevant to process economics, cost and throughput. Based on the selection of criteria studied as part of the Monte Carlo simulations, “Design Space 2” would be superior when the choice is driven by aspects of process robustness and maximizing productivity.

5.7 Conclusions

Early-stage bioprocess development faces the challenge of proposing operating conditions that are optimal, or at least close-to-optimal with limited resource and starting from minimal or no process knowledge. In this study, a simplex-based hybrid optimization approach was used to identify optimal operation parameters for the non-trivial separation of a pharmaceutical antibody in a three-component system with CEX chromatography. The optimization had to consider large ranges of the operational inputs loading, slope and initial salt concentration of the elution gradient to an extent that the process became subject to the physical constraint of product breakthrough.

As with any multi-objective optimization problem, the ultimate optimal conditions depend on the metrics chosen. Here, we focused on the optimization of product mass per cycle time with constraints for purity and yield as can be seen in Figures 3, 5, and 6. This metric was chosen to demonstrate major trade-offs between mass and time with opposite tendencies. For more traditional optimization problems where mass is often the only objective function (with some restrictions for purity and yield) the optimization of the

investigated separation could be reduced to high loading as the most influential input. By including time in the objective function in order to propose a more realistic trade-off regarding overall process productivity, the high salt regime had to be studied, along with areas of high loading. This revealed some interesting physico-chemical phenomena of the separation; BT was a natural consequence of the high salt and high loading conditions, however, the degree of control imposed by BT was unexpected.

The combination of the structured and logic-based simplex method with local fitting gave the method the exploratory character that led to the discovery of the physical process boundary of product BT and facilitated the dynamic and efficient generation of a large knowledge space. Such flexible workflows are enabled by the iterative and interactive nature of the simplex. In the studied separation where the optimum was highly controlled by the BT constraint, the simplex rapidly identified a direction of high potential whilst the process constraints could be outlined efficiently with local fitting. The contributions of both elements in the hybrid approach as part of a sequential workflow is discussed conceptually. In the center of this discussion is the exploitation of all process information in a data-driven holistic approach.

Through probabilistic analysis the knowledge space was made accessible and supported the investigation of optimal and robust design spaces. Monte Carlo simulations gave insight into the trade-offs of the process outputs, dominated by productivity and yield, and enabled the discussion of risk and reward of crossing the BT boundary. This led to the definition of a robust design space for 51 ± 3 g/ L_{resin} loading, 130 ± 10 mM initial salt and 20 ± 5 mM/CV slope of the elution gradient, producing 22.9 g/(h L_{resin}) of 95 % pure product with average yields of 68.5 %. This level of information is not typically available in early phase process development where times lines are usually tight and design space definitions often crude. As the molecule progresses to later stages of process development, the demand for material increases as does the need to demonstrate comprehensive process knowledge to support regulatory filing. The simplex-based hybrid approach facilitates vital process information to be gained early on in the development of bioprocessing unit operations, that can provide an advantage and potentially impact all later development stages.

Acknowledgments

The financial support for an Engineering Doctorate (EngD) from GlaxoSmithKline and the Engineering and Physical Science Research Council (EPSRC) of the United Kingdom for V. Fischer is duly appreciated.

V. Velayudhan acknowledges a Manufacturing Fellowship from the EPSRC.

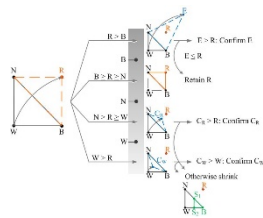
The initial DoE outline was produced in discussion with Sophie Russell of GlaxoSmithKline; her input is greatly appreciated.

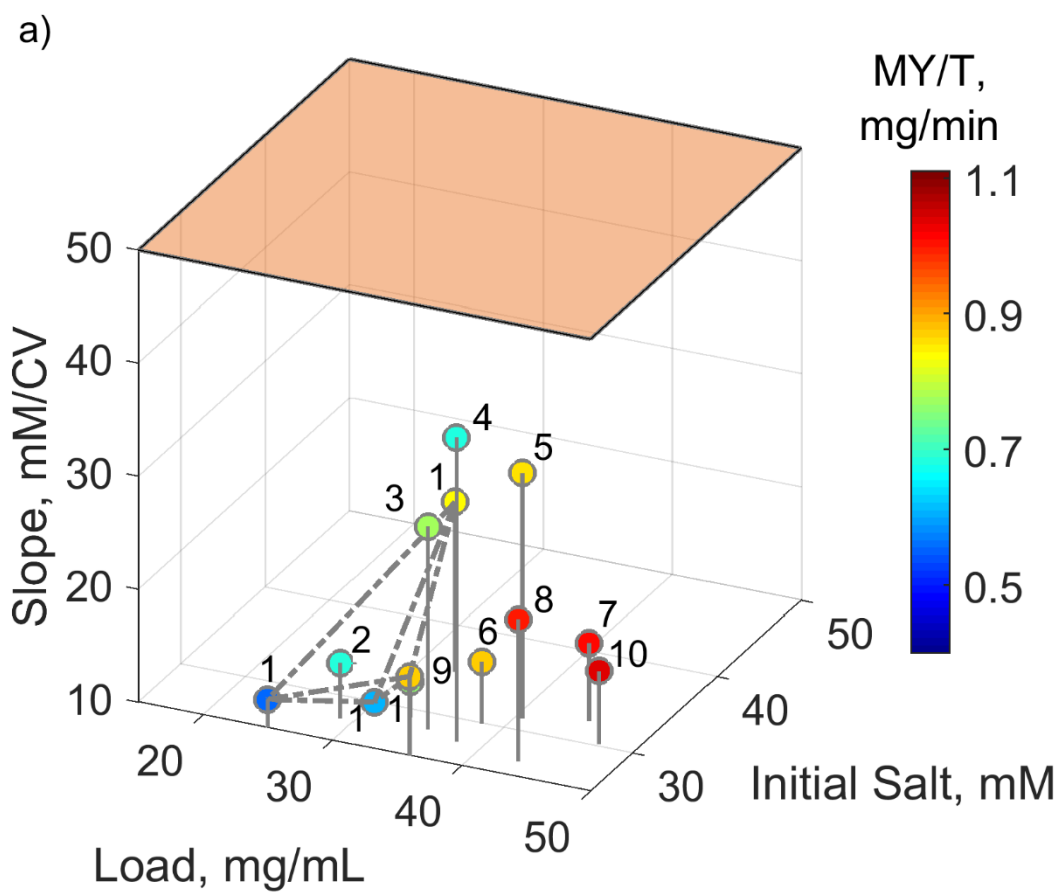
4. References

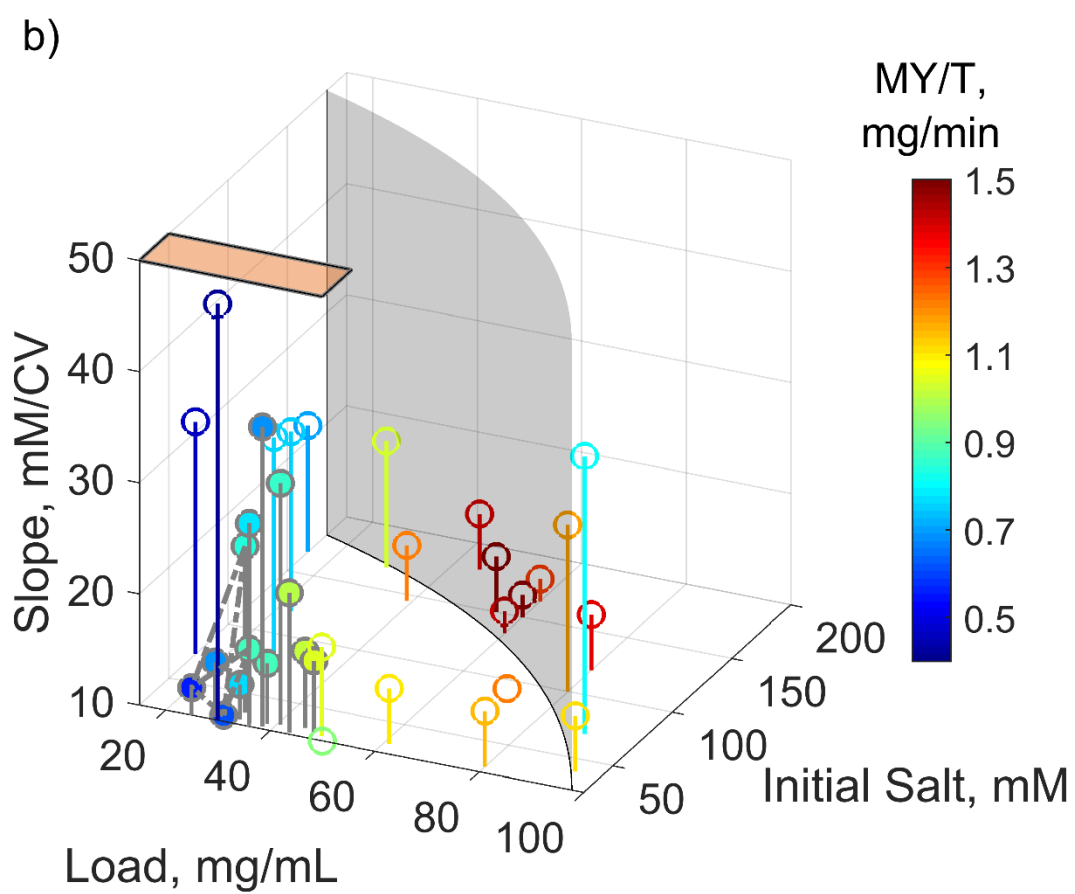
1. Welsh JP, Rauscher MA, Bao H, et al. Domain antibody downstream process optimization: High-throughput strategy and analytical methods. *Eng. Life Sci.* 2016;16(2):133-142.
2. Petroff MG, Bao H, Welsh JP, et al. High throughput chromatography strategies for potential use in the formal process characterization of a monoclonal antibody. *Biotechnology and Bioengineering.* 2016;113(6):1273-1283.
3. Kumar V, Rathore AS. Two-stage chromatographic separation of aggregates for monoclonal antibody therapeutics. *Journal of Chromatography A.* 2014;1368:155-162.
4. Borg N, Brodsky Y, Moscariello J, et al. Modeling and robust pooling design of a preparative cation-exchange chromatography step for purification of monoclonal antibody monomer from aggregates. *Journal of Chromatography A.* 2014;1359:170-181.
5. Xu Z, Li J, Zhou JX. Process development for robust removal of aggregates using cation exchange chromatography in monoclonal antibody purification with implementation of quality by design. *Preparative Biochemistry and Biotechnology.* 2012;42(2):183-202.
6. Khalaf R, Heymann J, LeSaout X, Monard F, Costioli M, Morbidelli M. Model-based high-throughput design of ion exchange protein chromatography. *Journal of Chromatography A.* 2016;1459:67-77.
7. Kateja N, Kumar D, Godara A, Kumar V, Rathore AS. Integrated Chromatographic Platform for Simultaneous Separation of Charge Variants and Aggregates from Monoclonal Antibody Therapeutic Products. *Biotechnol. J.* 2017;12(11).
8. Vetter TA, Ferreira G, Robbins D, Carta G. Predicting Retention and Resolution of Protein Charge Variants in Mixed-Beds of Strong and Weak Anion Exchange Resins with Step-Induced pH Gradients. *Sep. Sci. Technol.* 2014;49(12):1775-1786.
9. Close EJ, Salm JR, Bracewell DG, Sorensen E. Modelling of industrial biopharmaceutical multicomponent chromatography. *Chem. Eng. Res. Des.* 2014;92(7):1304-1314.
10. Huuk TC, Hahn T, Osberghaus A, Hubbuch J. Model-based integrated optimization and evaluation of a multi-step ion exchange chromatography. *Separation and Purification Technology.* 2014;136(0):207-222.
11. Nfor BK, Zuluaga DS, Verheijen PJT, Verhaert PDEM, Van der Wielen LAM, Ottens AM. Model-based rational strategy for chromatographic resin selection. *Biotechnology Progress.* 2011;27(6):1629-1643.
12. Freier L, von Lieres E. Multi-objective global optimization (MOGO): Algorithm and case study in gradient elution chromatography. *Biotechnol. J.* 2017;12(7).
13. Łacki KM. High throughput process development in biomanufacturing. *Current Opinion in Chemical Engineering.* 2014;6:25-32.
14. Kelley B, Blank G, Lee A. Downstream processing of monoclonal antibodies: Current practices and future opportunities. In: Gottschalk U, ed. *Process scale purification of antibodies.* New Jersey, US: John Wiley and Sons; 2008:1-23.
15. Guiochon G, Beaver LA. Separation science is the key to successful biopharmaceuticals. *Journal of Chromatography A.* 2011;1218(49):8836-8858.

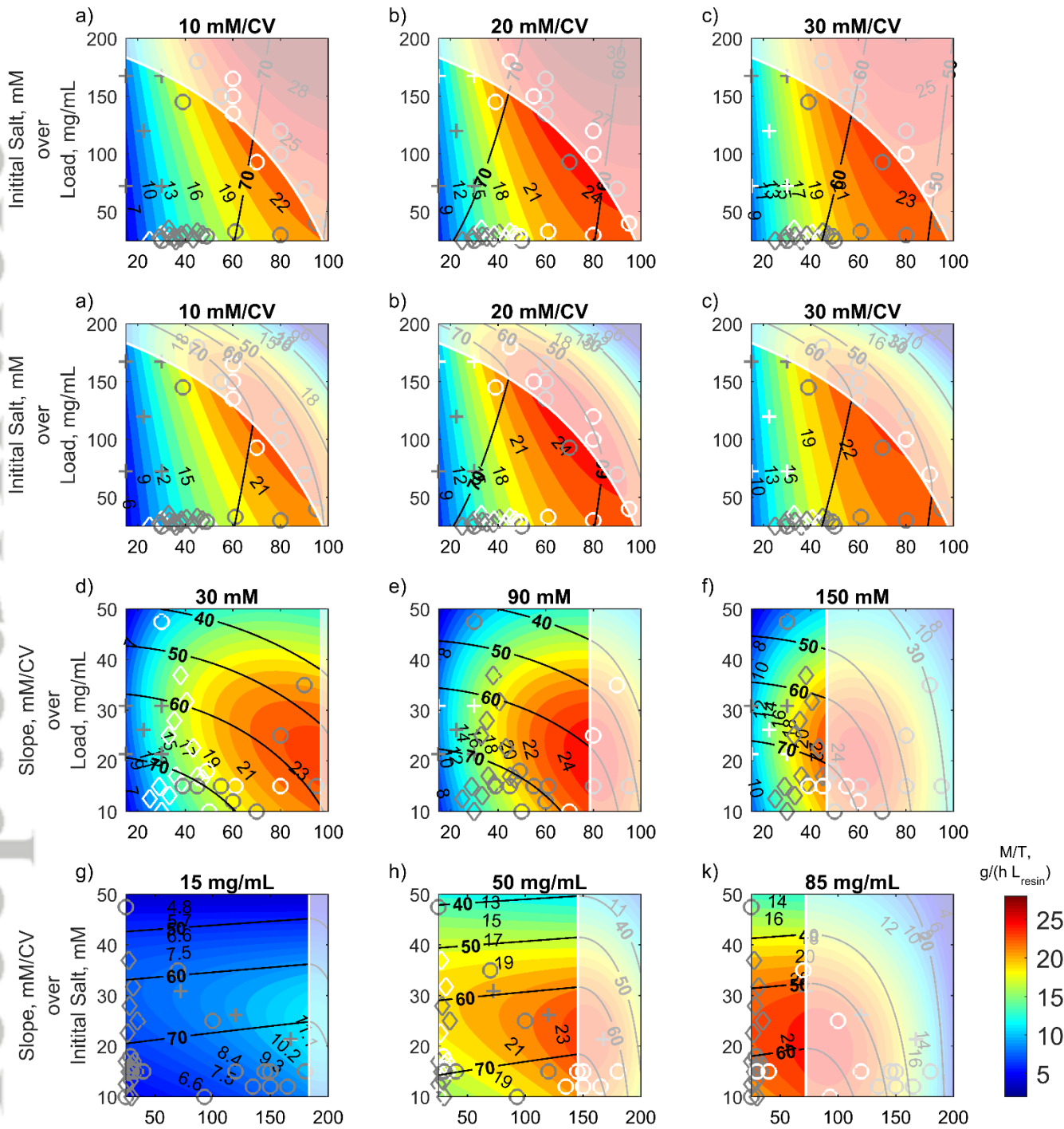
16. Spendley W, Hext GR, Himsworth FR. Sequential Application of Simplex Designs in Optimisation and Evolutionary Operation. *Technometrics*. 1962;4(4):441-461.
17. Nelder JA, Mead R. A Simplex Method for Function Minimization. *The Computer Journal*. 1965;7(4):308-313.
18. Ferreirós N, Iriarte G, Alonso RM, Jiménez RM. MultiSimplex and experimental design as chemometric tools to optimize a SPE-HPLC-UV method for the determination of eprosartan in human plasma samples. *Talanta*. 2006;69(3):747-756.
19. Watson MW, Carr PW. Simplex algorithm for the optimization of gradient elution high-performance liquid chromatography. *Analytical Chemistry*. 1979;51(11):1835-1842.
20. Berridge JC. Simplex optimization of high-performance liquid chromatographic separations. *Journal of Chromatography A*. 1989;485(0):3-14.
21. Drgan V, Kotnik D, Novič M. Optimization of gradient profiles in ion-exchange chromatography using computer simulation programs. *Anal. Chim. Acta*. 2011;705(1):315-321.
22. Bezerra MA, dos Santos QO, Santos AG, Novaes CG, Ferreira SLC, de Souza VS. Simplex optimization: A tutorial approach and recent applications in analytical chemistry. *Microchemical Journal*. 2016;124:45-54.
23. Viader-Salvadó JM, Castillo-Galván M, Fuentes-Garibay JA, Iracheta-Cárdenas MM, Guerrero-Olazarán M. Optimization of five environmental factors to increase beta-propeller phytase production in *Pichia pastoris* and impact on the physiological response of the host. *Biotechnology Progress*. 2013;29(6):1377-1385.
24. Konstantinidis S, Chhatre S, Velayudhan A, Heldin E, Titchener-Hooker N. The hybrid experimental simplex algorithm - An alternative method for 'sweet spot' identification in early bioprocess development: Case studies in ion exchange chromatography. *Anal. Chim. Acta*. 2012;743:19-32.
25. Konstantinidis S, Titchener-Hooker N, Velayudhan A. Simplex-based optimization of numerical and categorical inputs in early bioprocess development: Case studies in HT chromatography. *Biotechnol. J*. 2017;12(8).
26. Steinhauser MO. Introduction to MC Simulation. *Computer simulation in physics and engineering*. Boston, US: De Gruyter; 2013.
27. Pardoux É. Simulations and the Monte Carlo method. *Markov processes and applications: algorithms, networks, genome and finance*. Chichester, UK: John Wiley & Sons, Ltd; 2010.
28. Konstantinidis S, Welsh JP, Roush DJ, Velayudhan A. Application of simplex-based experimental optimization to challenging bioprocess development problems: Case studies in downstream processing. *Biotechnology Progress*. 2016;32(2):404-419.
29. Walters FH, Parker Jr. LR, Morgan SL, Deming SN. *Sequential simplex optimisation: a technique for improving quality and productivity in research, development, and manufacturing*. Florida, US: CRC Press; 1991.

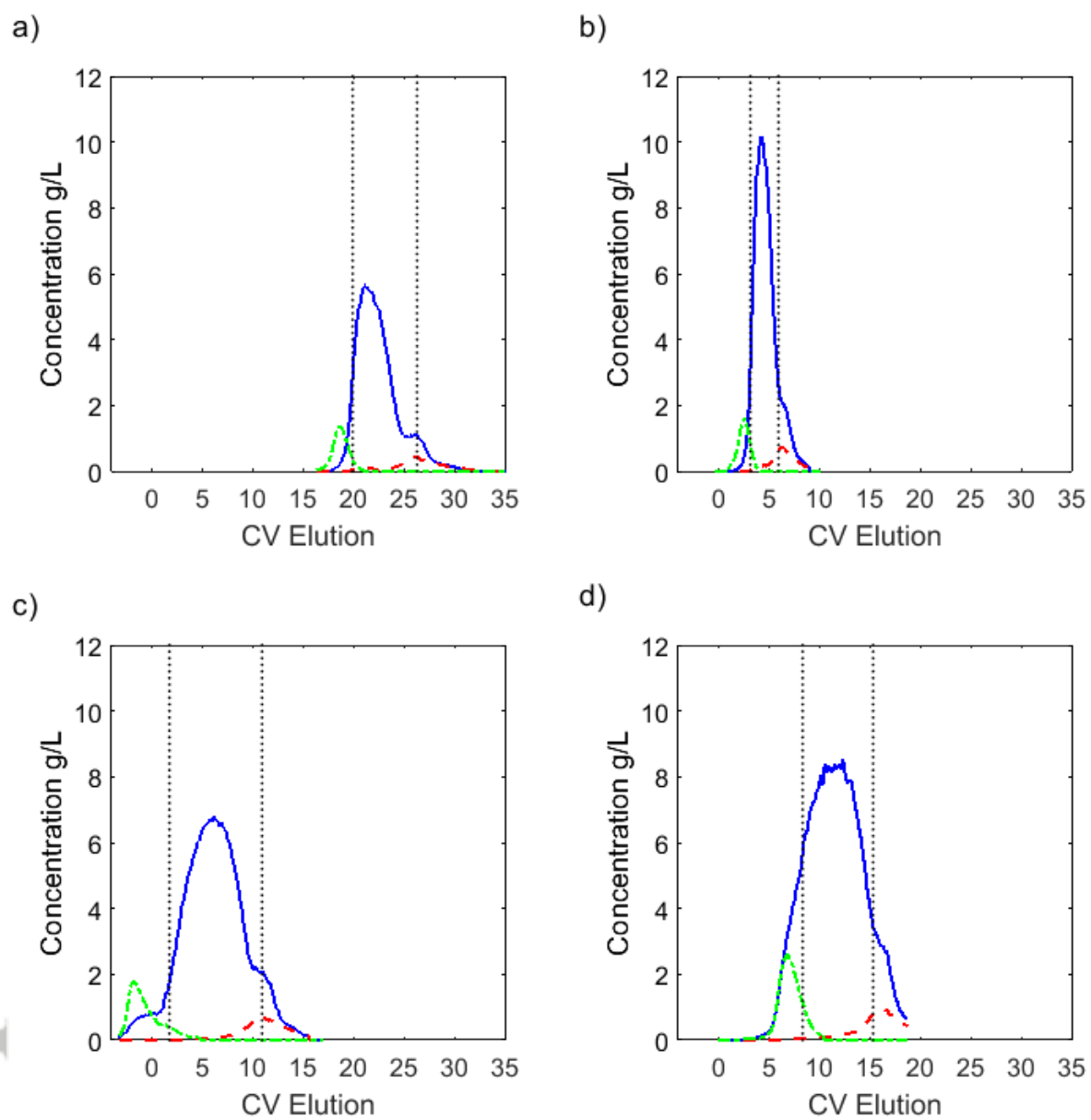
Figure 1. Schematic illustration of the simplex rules and movements during an iteration for maximization of the objective function. – Two-dimensional space with three input variables. Vertexes in the simplex are sorted from “best” (B) via “next-to-the-worst” (N) to “worst” (W) with regards to their objective function values. After “reflection” (R) subsequent moves might be suggested, i.e. “expansion” (E), “outside contraction” (C_R), “inside contraction” (C_W) and “shrinkage” (S).











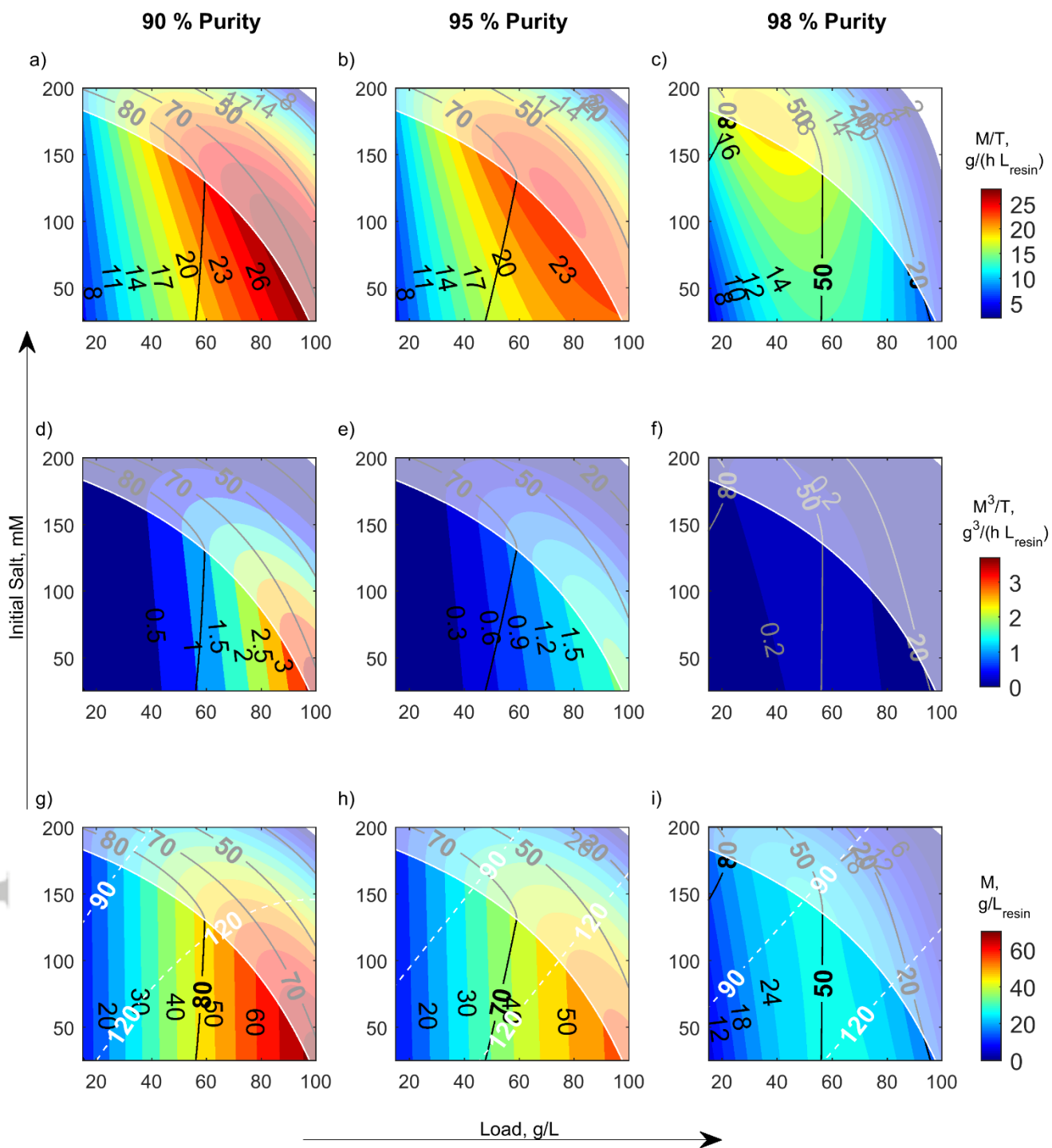


Table 1. Measured points of the central composite design matrix.

Design Point Type	Loading in g/L	Initial Salt in mM	pH
Factorial	15.0	72.5	5.0
Factorial	30.0	72.5	5.0
Axial	22.5	120.0	5.0
Factorial	30.0	167.5	5.0
Factorial	15.0	167.5	5.0

Table 2. Monte Carlo simulation results for optimal design spaces subject to different acceptance criteria. – Risk describes the permitted number of failures for a specified yield (Y) constraint and the occurrence of product breakthrough (BT) at an upper limit of 5 % BT. Presented are median values for 1000 simulations per design space.

Design Space Specifications	Acceptance Criteria	Violations	Yield in %	Mass in mg	Time in min	Productivity in g/(h L _{resin})
Initial Design Space: [15 ± 3 g/L, 145 ± 10 mM, 20 ± 5 mM/CV]	≥ 70 % Yield	27 % (Yield)	70.7 (≥ 66.2)	140	82	20.5
Design Space 1: [24 ± 3 g/L, 165 ± 10 mM, 20 ± 5 mM/CV]	≥ 70 % Yield 2 % Risk	0.9 % (Yield) 0.1 % (BT)	72.5 (≥ 68.8)	89 (-37 %)	69 (-19 %)	15.4 (-25 %)
Design Space 2: [51 ± 3 g/L, 130 ± 10 mM, 20 ± 5 mM/CV]	≥ 65 % Yield 0 % Risk	None	68.5 (≥ 65.0)	175 (+26 %)	92 (+11 %)	22.9 (+12 %)
Design Space 3: [72 ± 3 g/L, 120 ± 10 mM, 20 ± 5 mM/CV]	No Y Constraint 100 % Risk	100 % (BT)	63.0 (≥ 59.2)	224 (+60 %)	106 (+23 %)	25.3 (+23 %)